Design of a neutron detector

Thomas Baumann

National Superconducting Cyclotron Laboratory
Michigan State University
e-mail: baumann@nscl.msu.edu

February 22, 2001

1 Introduction

The scope of this project is to design and build a neutron detector to be used in connection with the new sweeper magnet and the S800 magnetic spectrograph. The existing neutron walls [1] have a deficiency in detection efficiency, which is 20% for neutrons of roughly 20 MeV, but drops to only 12% for neutrons of 50 MeV or more. This limits their use to low energy beams and low multiplicity experiments.

The new neutron wall should have a higher detection efficiency, especially for higher energies of up to 300 MeV. It should work as a time-of-flight wall, i.e. the neutron energy is measured through the time-of-flight instead of the energy deposition in the detector. To accommodate for a long flight path and a good angular coverage, the detector area should measure about 2×2 m^2. This should match the sweeper magnet's gap size.

The basic idea is to follow the design of GSI's LAND array, which utilizes plastic scintillator sheets in a combination with iron converters [2]. The reason for using iron is that the nuclear interaction length (at high particle energies) for this material is only around 17 cm, while it is 80 cm for plastic. If the amount and distribution of iron layers between the scintillator layers is chosen correctly, the overall thickness of the detector can be reduced while maintaining a high detection efficiency. This has to be optimized for the energy range the detector should work in.

2 Simulation

A detailed simulation is needed to optimize the detector design for the given energy range and to ensure that the detector will meet anticipated specifications.

I started out using CERN's detector development tool GEANT [3]. The LAND collaboration discarded GEANT because another Monte Carlo Code,

HETC, yielded a better description of measured efficiencies [2]. Unfortunately, HETC is currently not available. Therefore one of the tasks is to adapt GEANT to the given problem.

2.1 How the efficiency curve is calculated

Using GEANT, I can calculate the complete efficiency curve for a given range of neutron energies in one step. The energy of the incoming neutrons is randomly distributed within the given range of energies (usually from 0 to $E_{\max}$). Two histograms with identical binning are booked at the initialization. One records the energies of all incoming neutrons. The other only records the energies of those neutrons which are detected. At the end of each event, a third histogram is created by dividing the two histograms that were filled throughout the event. The resulting histogram directly yields the efficiency curve, independently of the actual distribution of incoming energies. Error bars according to the statistics accumulated are also calculated. The rest of the GEANT calculation is merely for determining if a neutron is detected or not.

2.2 Comparison of GEANT efficiency calculations with measurements and other programs

The first step of checking a simulation routine is to compare it to existing measurements and to other available simulation programs.

In the case of GEANT, there are three different packages that are tailored for hadronic interactions and neutron detection. These are GEISHA, the hadronic interaction package, FLUKA, an addition from the stand-alone version of FLUKA [4], and MICAP, which extends GEISHA by added cross sections for neutrons below 20 MeV.

2.2.1 First round of GEANT simulations

For the first round of GEANT simulations, the results were compared to measured data from Ref. 5, the HETC simulation published in Ref. 2, and to simulations from the KSUVAX code.

The Cecil data [5] only contain efficiency curves for pure scintillator material. So a comparison of the scintillator-iron combination can only be done with the HETC efficiency curves from the LAND paper [2].

On the GEANT side, usually the GEISHA/MICAP combination was used. The light output was calculated using GEANT's `GBIRK` routine that computes the electron equivalent energy for each energy step according to Birks' saturation law. Details are given in the GEANT manual, section `PHYS337`.

The first comparison is shown in Fig. 1. Here, a NE-102 scintillator of 30.5 cm by 12.7 cm diameter was bombarded with neutrons ranging from 20 to 180 MeV. Three different threshold settings for the light output in

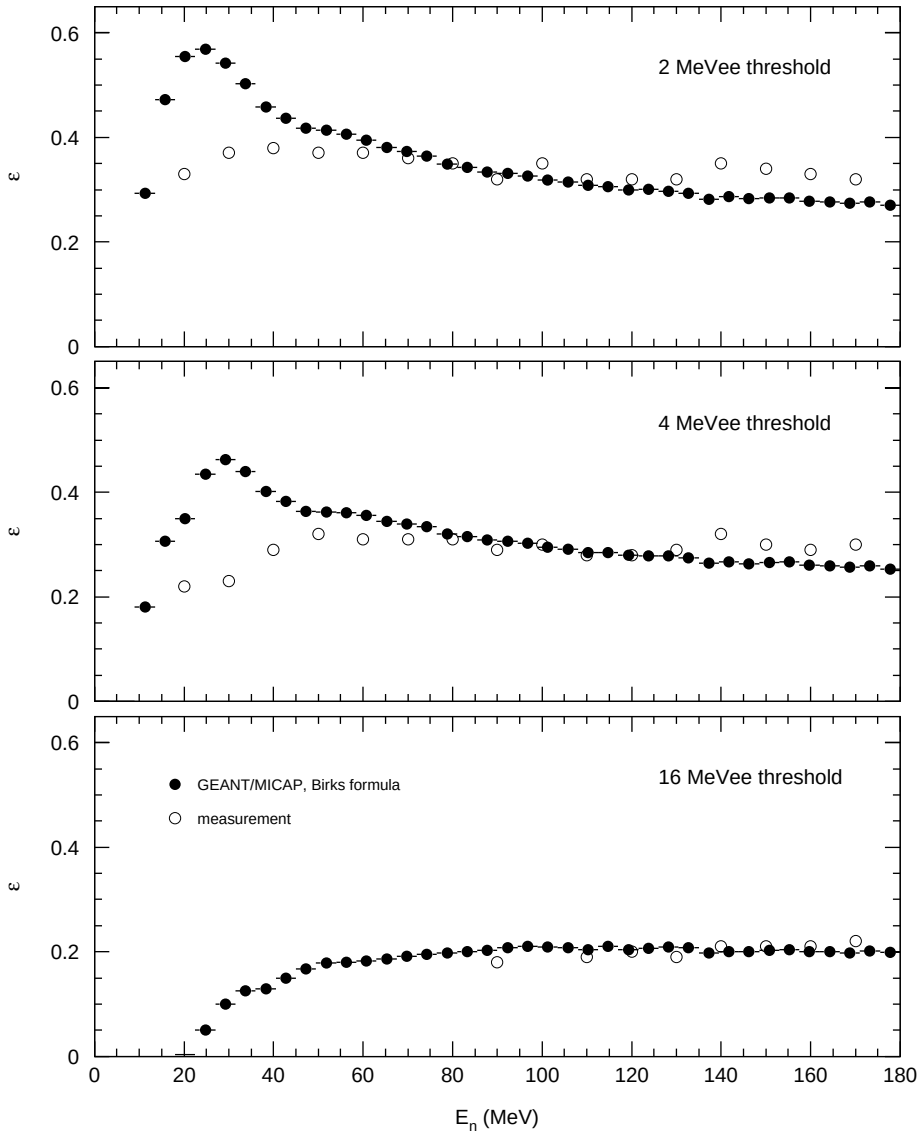

Figure 1: The three plots show a comparison of the efficiency of a 30.5 cm by 12.7 cm in diameter NE-102 scintillator, as measured for neutrons ranging in energy from 20–180 MeV [5] and as calculated by GEANT/MICAP. Three different settings for the threshold are compared.

electron equivalent energy were used. While the GEANT simulation reproduces the efficiency curve nicely at higher energies, there is a considerable over-prediction between 10 and 50 MeV for the lower threshold settings.

Another data set from the Cecil paper gives an efficiency curve for the energy range of 5 to 40 MeV, see Fig. 2. The measurement was done using a 5.08 cm by 10.27 cm in diameter NE-102 scintillator. Two threshold settings are compared. While the efficiency at the highest energy of 50 MeV is nicely reproduced for both thresholds, the calculated efficiency from GEANT is again too high at energies between 10 and 40 MeV.

Figure 3 shows a comparisons of efficiency curves for the 0–300 MeV energy range. These curves are all calculations for a $200 \times 200 \times 20$ cm^3 pure plastic scintillator. The different codes used are: HETC, data taken from the LAND publication, KSUVAX, a code that was modeled to reproduce measured efficiency curves for organic scintillators, and GEANT/FLUKA. Also here there's a discrepancy between the GEANT calculation and other codes at low energies.

In Fig. 4, efficiency curves from HETC and GEANT for the energy range of 0–1000 MeV are plotted, again for a $200 \times 200 \times 20$ cm^3 pure plastic scintillator. The overall agreement seems to be good, because GEANT's over-prediction at energies below 50 MeV is no longer resolved.

The simulations for the sandwich structure of plastic scintillator combined with iron look different, and here the discrepancies between GEANT and HETC are even larger. There are only very few experimental data available (see Fig. 19) and the KSUVAX code can not handle other materials than scintillator, so here only a comparison with the HETC results taken from the LAND paper is done. The HETC efficiency curve for a $200 \times 200 \times 20$ cm^3 detector in sandwich structure with 5 mm iron and 5 mm scintillator layers is plotted together with three different GEANT calculations in Fig. 5. The introduction of the iron converter increased the discrepancy between HETC and GEANT even more. The GEANT calculations yield to high an efficiency for energies below about 400 MeV, which is just the range that we are interested in.

2.2.2 Improved second round of GEANT calculations

I looked for differences between my GEANT-code and one used by Sally Gaff and Lilian Martin for the simulation of the existing neutron walls. One main difference was the calculation of the light output in electron equivalent energies. While I previously used Birks saturation law (built into the routine `GBIRK`), Sally's code sports Madey's formula, which can be found in Cecil's paper [5].

However, there is a basic difference in the two formulas in the way the

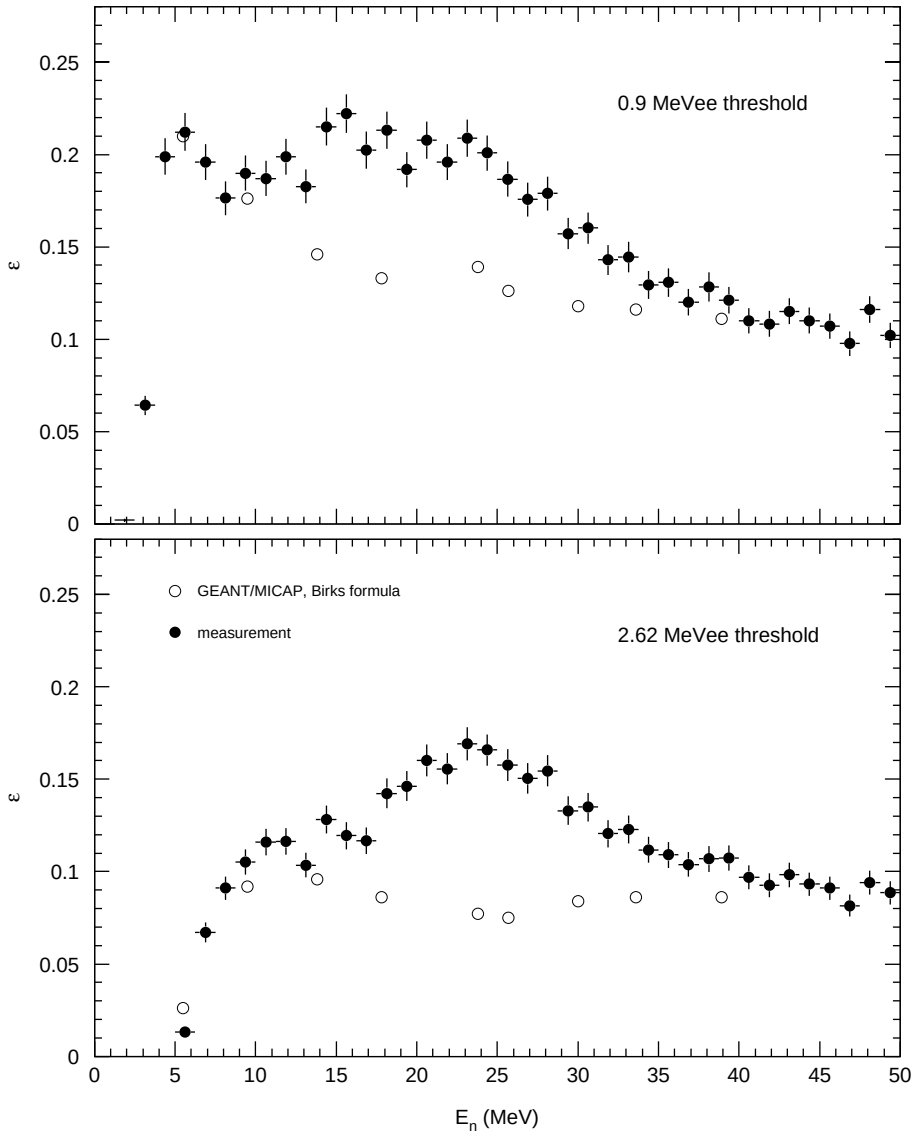

Figure 2: Comparison of the efficiency of a 5.08 cm by 10.27 cm in diameter NE-102 scintillator, as measured for neutrons ranging in energy from 5–40 MeV and as calculated by GEANT/MICAP. Two different settings for the threshold are compared.

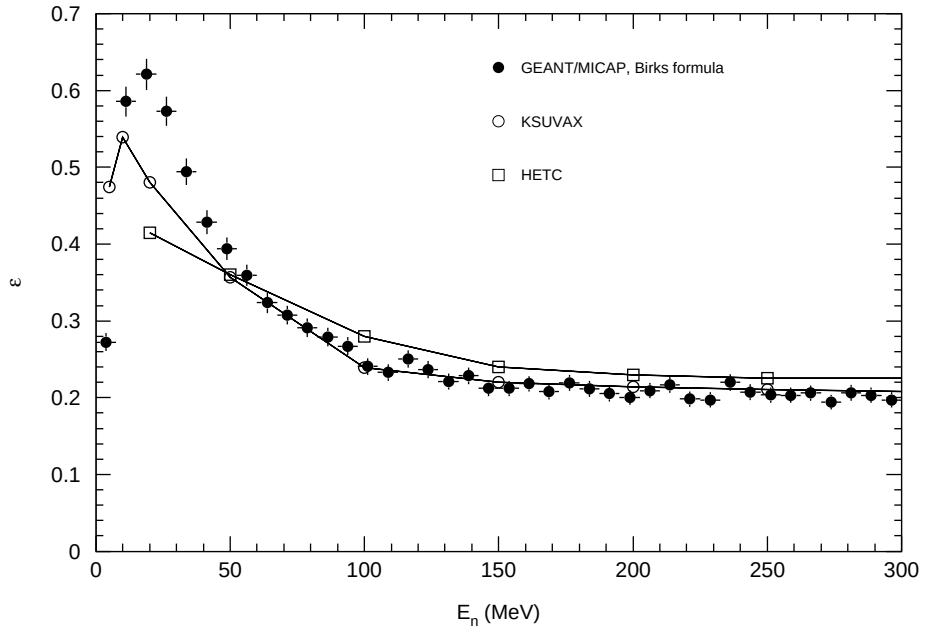

Figure 3: Comparison of detection efficiency for a $200 \times 200 \times 20$ cm^3 pure plastic scintillator as calculated by three different codes.

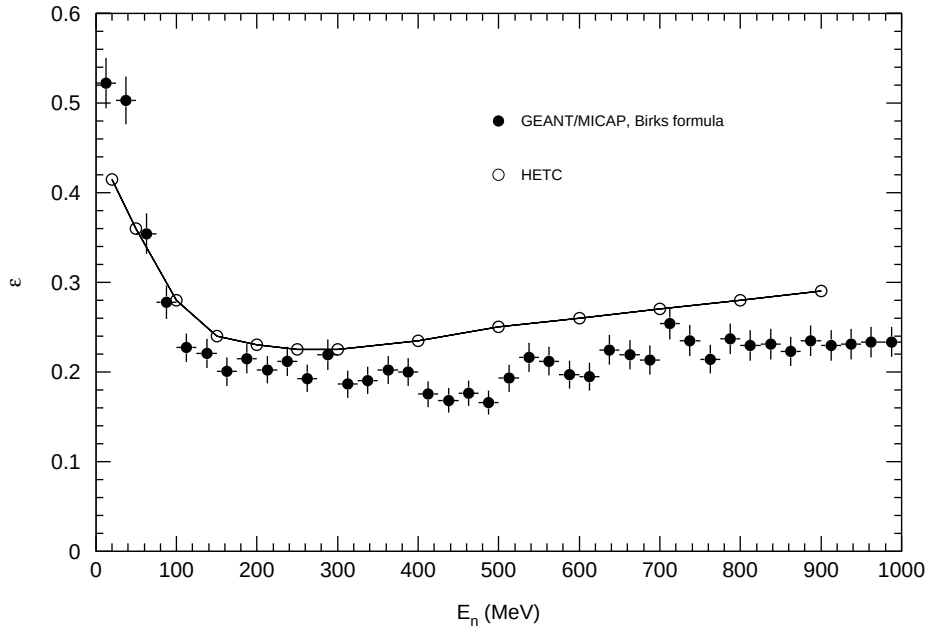

Figure 4: Efficiency curve for neutrons impinging on a $200 \times 200 \times 20$ cm^3 pure plastic scintillator.

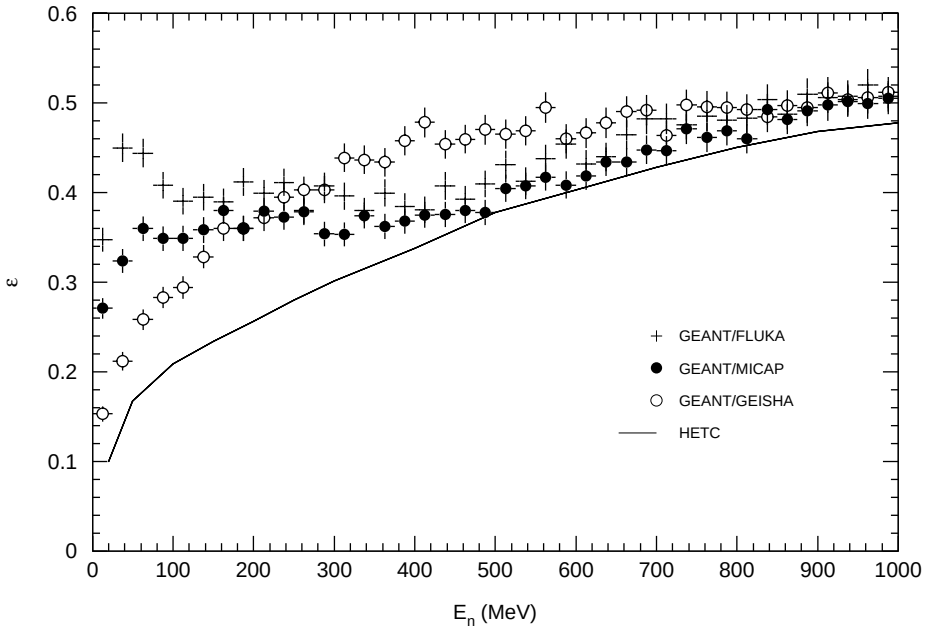

Figure 5: Detection efficiency as calculated by HETC and various GEANT flavors for a $200 \times 200 \times 20$ cm^3 detector in sandwich structure with 5 mm iron and 5 mm scintillator layers.

light output is calculated. Birks' formula

$$\frac{dL}{dx} = \frac{S\frac{dE}{dx}}{1 + kB\frac{dE}{dx} + C\left(\frac{dE}{dx}\right)^2} \tag{1}$$

(see Ref. 7, pp. 220–225) calculates the light output from the differential energy loss dE/dx. Here S is the normal scintillation efficiency and kB as well as C are treated as empirically fitted parameters. If dE/dx is known, the light output can easily be calculated for each little step (and energy loss) that the particle did, and the total light output can be summed up after the track is completed. In GEANT, the dE/dx are interpolated from tabulated values, and they are constant for each step Δx. Therefore, the integrated light output ΔL for one step is simply

$$\Delta L = \frac{S\Delta E}{1 + kB\frac{dE}{dx} + C\left(\frac{dE}{dx}\right)^2}\,, \tag{2}$$

with ΔE being the energy deposited during this step.

The formula that the routine `GBIRK` uses is actually slightly different in that the scintillation efficiency S is missing:

$$R = \frac{\Delta E}{1 + C_1\delta + C_2\delta^2}\,, \qquad \delta = \frac{1}{\rho}\frac{dE}{dx}\,. \tag{3}$$

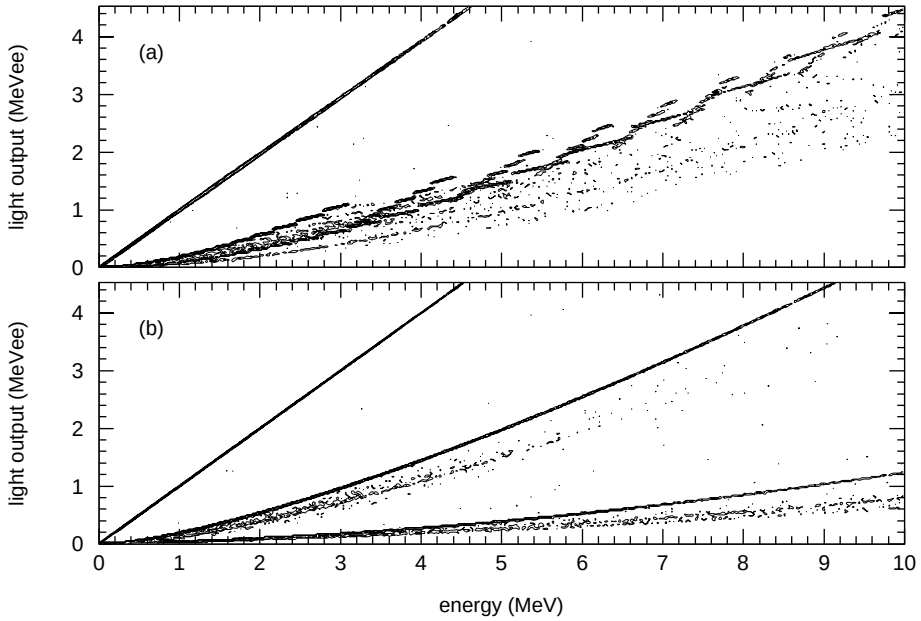

Figure 6: Panel (a) shows the light output for the various particles calculated by the `GBIRK` routine, model parameter 1 (high-charge correction on). The bottom panel (b) shows light output curves calculated with Madey's formula, Eq. 4. The three branches represent the light output for electrons, protons, and alpha particles (from top to bottom).

Since the scintillation efficiency is an arbitrary unit to compare different scintillation materials, it doesn't make a difference in this case. There is also a correction of the parameters C_1 and C_2 for particles with higher charges (see the GEANT manual). The light curves that are produced with `GBIRK` can be seen in Fig. 6 (a). Besides differences in the light amplitude, most notably for alpha particles, one can also see the effect of discrete dE/dx values, which produce discontinuities in the light output curves.

There is a correction built into the `GBIRK` routine for particles with charges equal or larger two. This correction reduces C_1 and therefore enhances the light output for these particles. According to the manual, this correction is needed for organic scintillators.

Comparing the light output curves of the `GBIRK` routine with the Madey curves, it seems that the light output for alpha particles needs to be decreased, rather than enhanced. Using a C_1 four times larger than for protons in fact gives results similar to those calculated using the Madey formula (See Fig. 8).

The other formula I used, following the example of Sally Gaff, is taken

from the Cecil paper [5]:

$$T_{\mathrm{e}} = a_1 T_{\mathrm{p}} - a_2 \left[1 - \exp\left(-a_3 T_{\mathrm{p}}^{a_4}\right)\right] : \tag{4}$$

here, T_{e} is the electron equivalent energy and T_{p} the proton energy. The parameters a_i are fitted to experimental data. For this formula to work correctly, the energy deposition by the charged particle has to be summed over the part of the track inside one detector volume prior to conversion. Also, parameter sets of a_i are only available for protons and alpha particles. The corresponding light output curves are plotted in Fig. 6 (b).

This different way of calculating the light output seems to work very well in fixing the over-prediction of efficiency at energies between 10 and 50 MeV. Also the different threshold settings are well-reproduced.

However, together with iron, the GEANT calculation still doesn't perform very well, compared to HETC, see Fig. 12. Figure 13 depicts the large discrepancy at energies below 400 MeV. Interestingly, for energies above 400 MeV, GEANT does a better job simulating the iron-plastic sandwich than the pure plastic scintillator.

2.2.3 Checking material dependence

One of the possible causes of the over-predicted efficiency at energies below 400 MeV could be hidden in the neutron cross sections that GEANT/MICAP uses. The total cross section of neutrons on ^{56}Fe from the `n-endf` database is shown together with the values extracted from the GEANT calculation (MICAP cross section table).

A comparison between tungsten and iron revealed an interesting dependence of the shape of the efficiency curve on the thickness of the converter material. Using 5 mm tungsten as converter instead of 5 mm iron results in an efficiency curve that drops off rapidly for low energies, very much like the HETC simulation does for iron (see Fig. 15). If the thickness of the tungsten is adjusted to get the efficiencies closer to what one gets for the iron, the efficiency for energies below 400 MeV doesn't decrease as much as it does for the higher energies. The same trend is seen for iron (Fig. 16). Now the question is, since the simulation is only compared with another simulation, if this is a physical effect or if it is a mistake of the simulation.

2.2.4 Variations of threshold and light collection, third round of calculations

Besides the details of particle tracking, cross sections and calculating the equivalent light output, other points can have a big impact on the detection efficiency, e.g., the way the threshold is applied. For an actual detector test or test experiment it is relatively simple to guess how the light is summed up and where the threshold applies. But if you want to compare with just

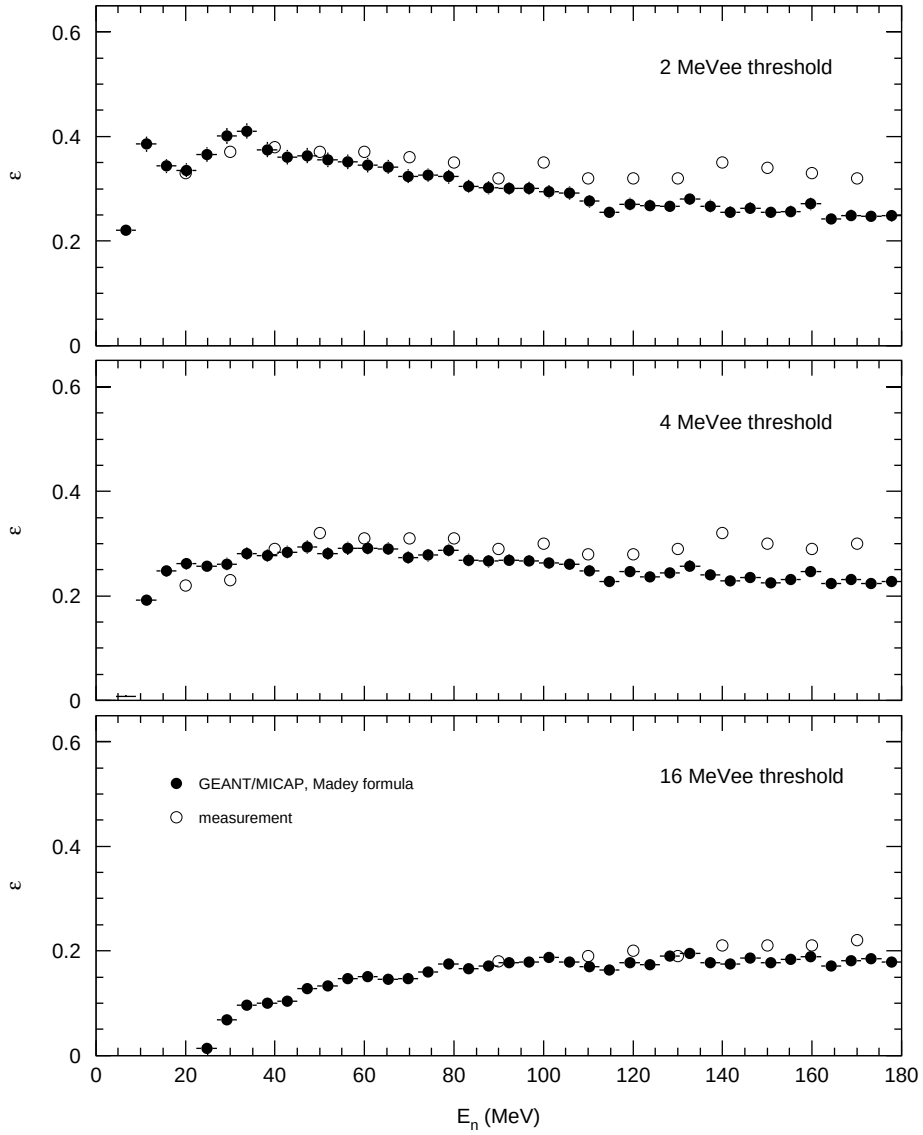

Figure 7: Comparison of measured efficiency curves with GEANT simulations using the Madey formula for the calculation of the light output. This is for a 30.5 cm by 12.7 cm diameter NE-102 scintillator. The over-prediction of efficiency in the 10–50 MeV range (see Fig. 1) is gone and the overall agreement is good.

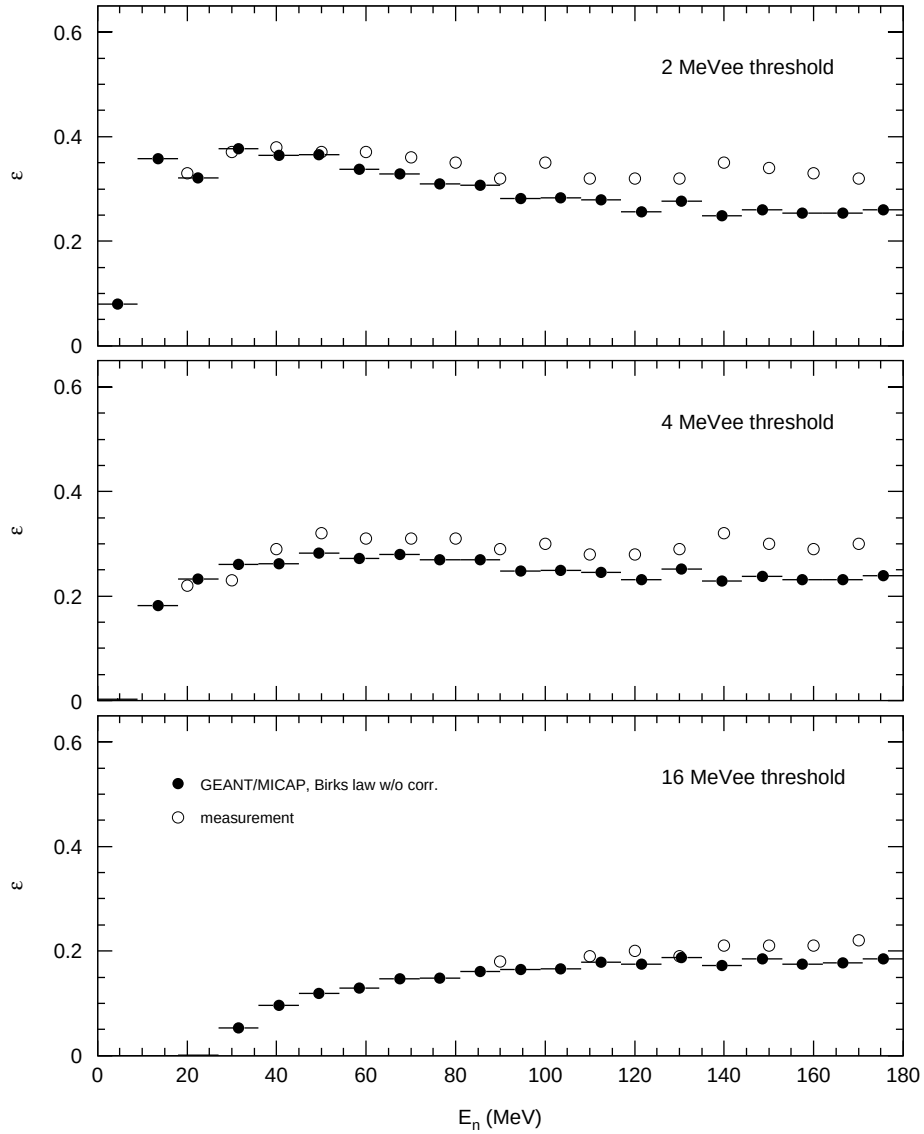

Figure 8: Comparison of measured efficiency curves with GEANT simulations using Birks law (routine `GBIRK` with modified response for alpha particles). This is for a 30.5 cm by 12.7 cm diameter NE-102 scintillator.

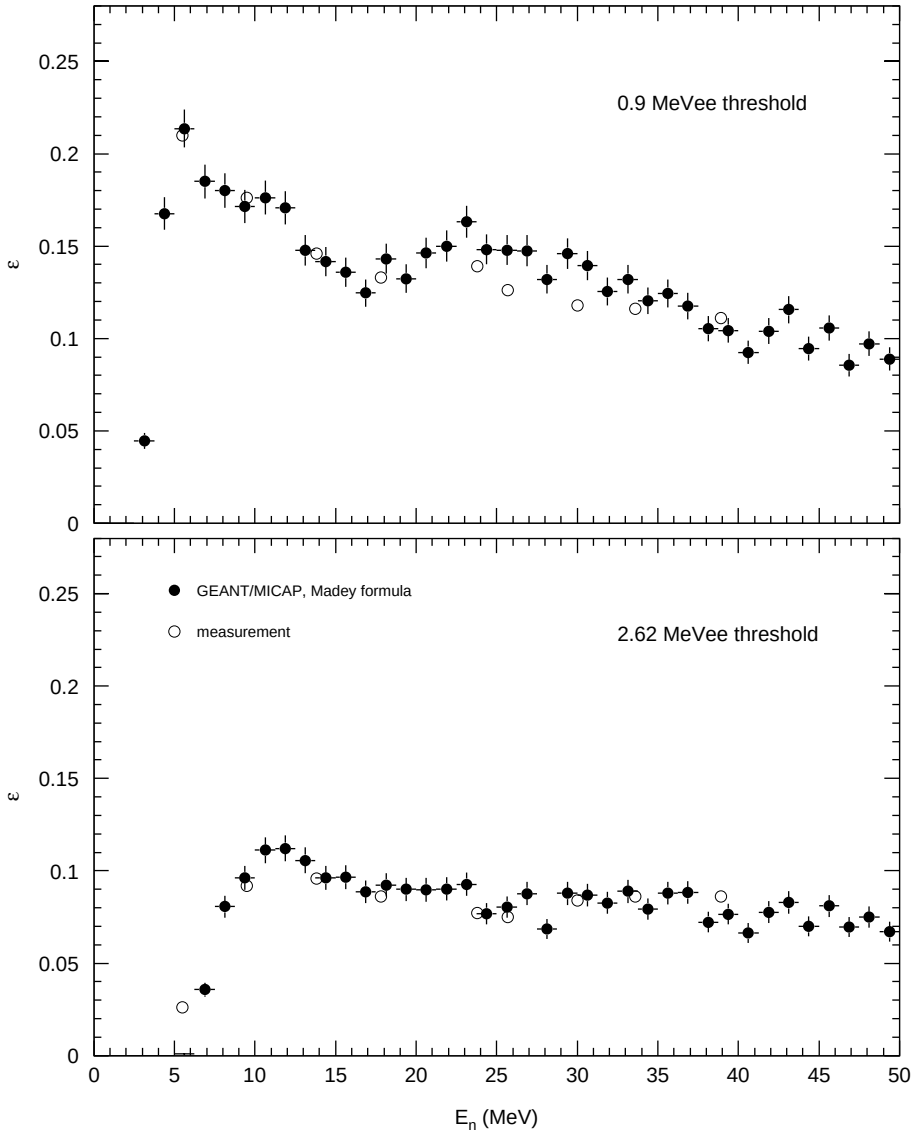

Figure 9: Comparison of the efficiency of a 5.08 cm by 10.27 cm diameter NE-102 scintillator. Also here the use of the Madey formula improves the agreement considerably compared to Fig. 2.

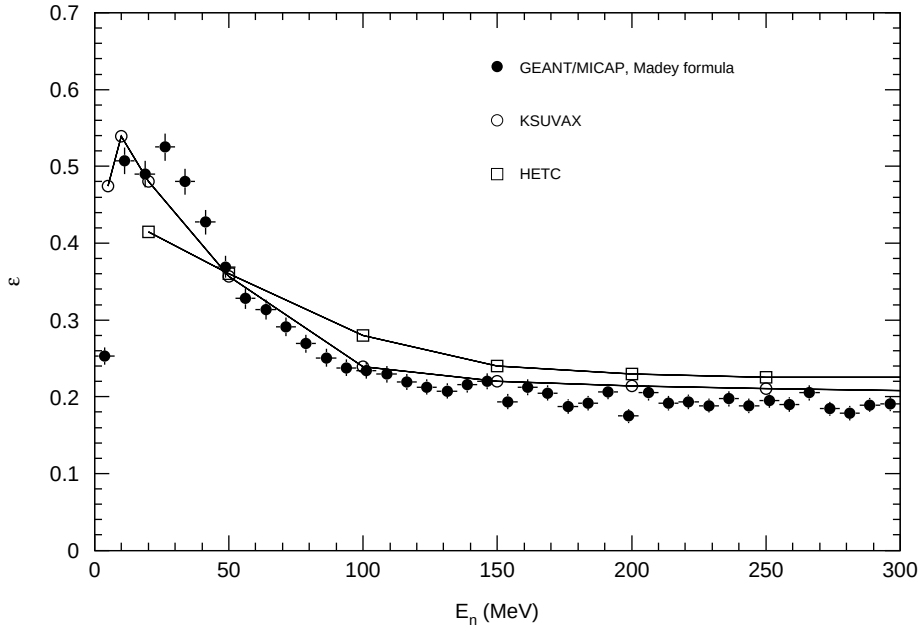

Figure 10: Detection efficiency curves for a $200 \times 200 \times 20$ cm^3 pure plastic scintillator. The agreement of the GEANT calculation with other codes at energies up to 300 MeV is still good.

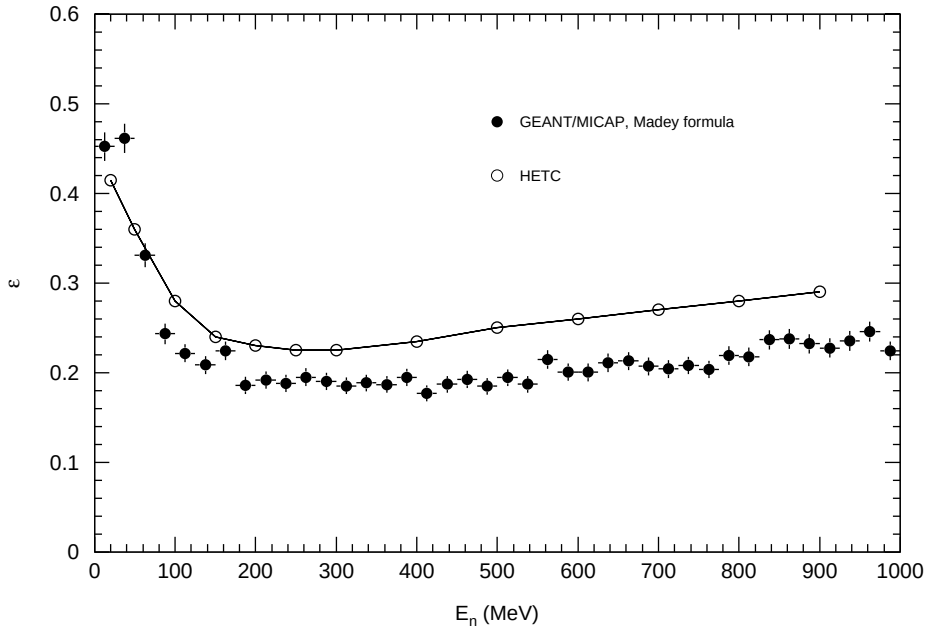

Figure 11: At energies up to 1000 MeV, the GEANT calculation yields slightly lower efficiencies than HETC. This trend seems to be a little bit stronger than with the previous calculation plotted in Fig. 4.

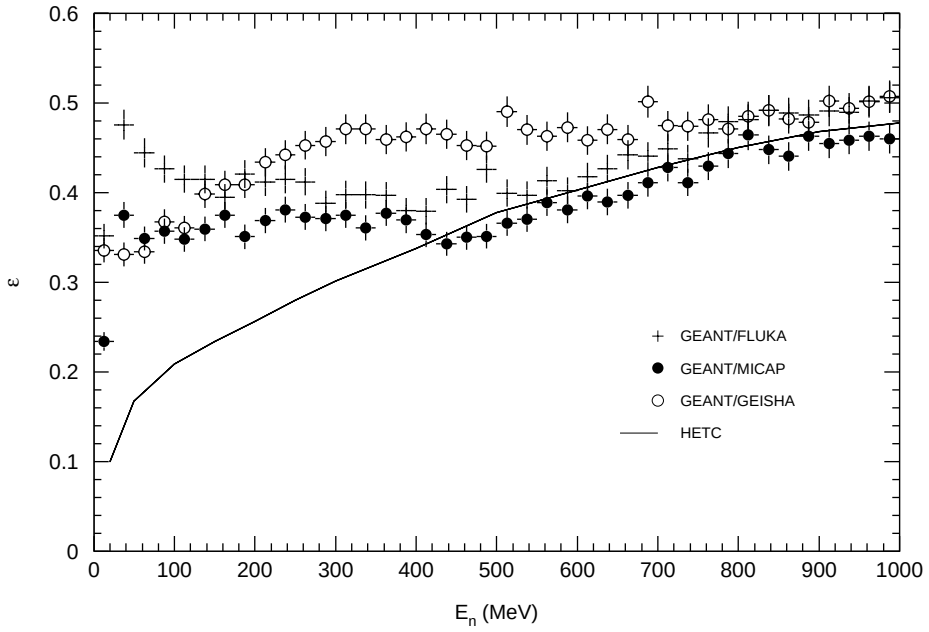

Figure 12: Adding iron to the detector, as here in a $200 \times 200 \times 20$ cm^3 sandwich structure of 5 mm iron and 5 mm scintillator layers, the simulation with Madey's formula shows no improvement over the simulation plotted in Fig. 5.

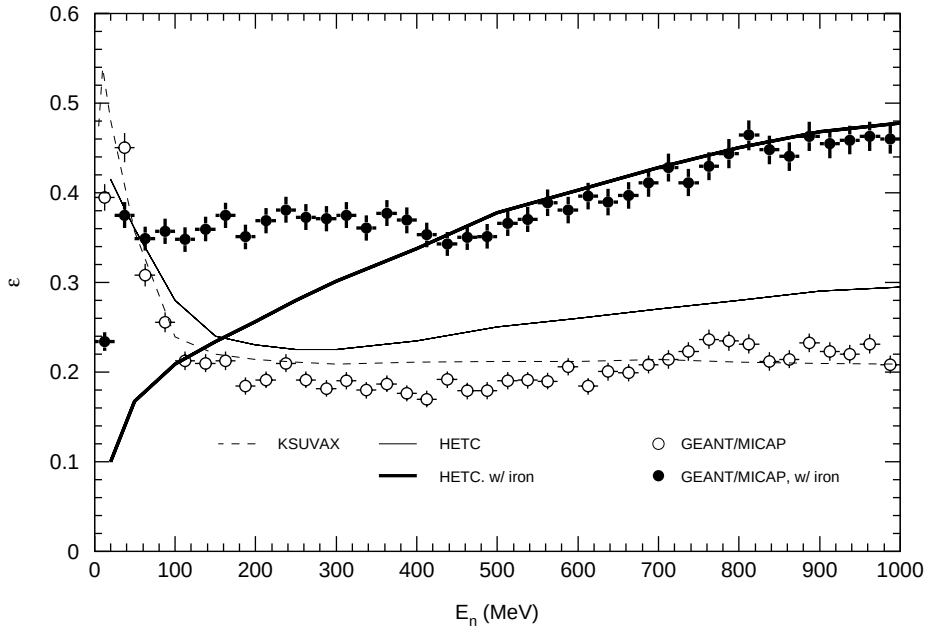

Figure 13: This plot shows how the pure scintillator structure's efficiency calculated by GEANT (open symbols) is right on top of the KSUVAX calculation (dashed) and follows the HETC simulation (thin line), while the sandwich structure of iron and plastic scintillator yields large discrepancies at neutron energies below 400 MeV (bold lines and filled symbols).

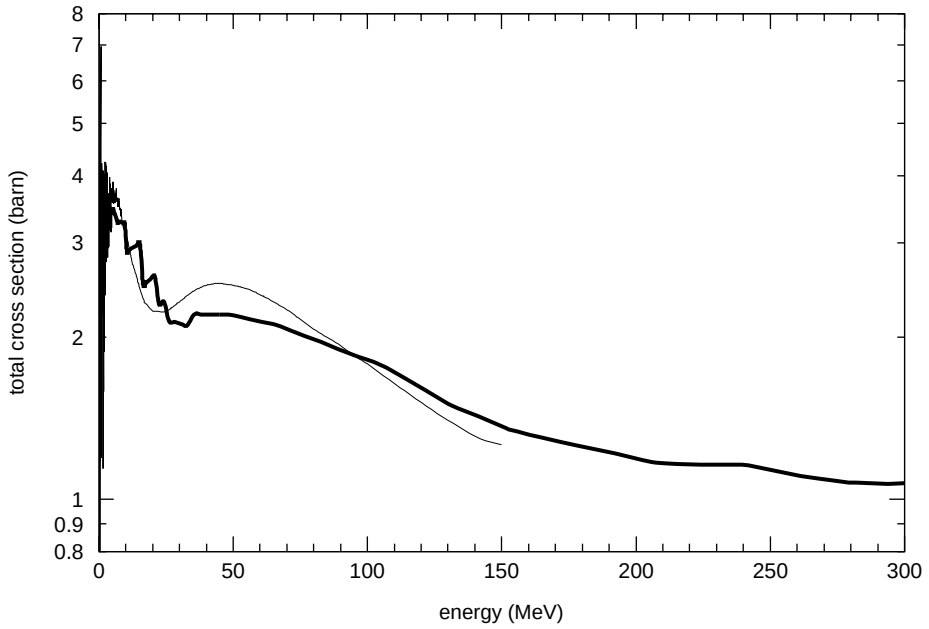

Figure 14: Total cross section of neutrons on ^{56}Fe. The thin line represents values taken from the `n-endf` data base, while the thick line are the GEANT cross section (in this case interpolated for the 0.1–1 GeV range).

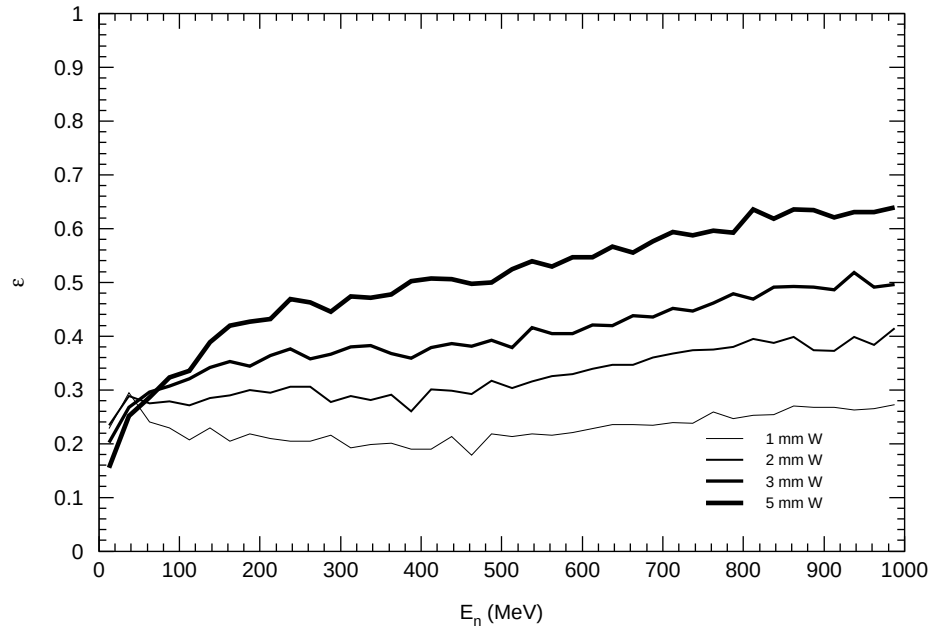

Figure 15: Efficiency curves for a 200×200 cm^2 sandwich structure consisting of 20 plastic scintillator sheets with 5 mm thickness each and 20 tungsten layers of different thicknesses (see legend).

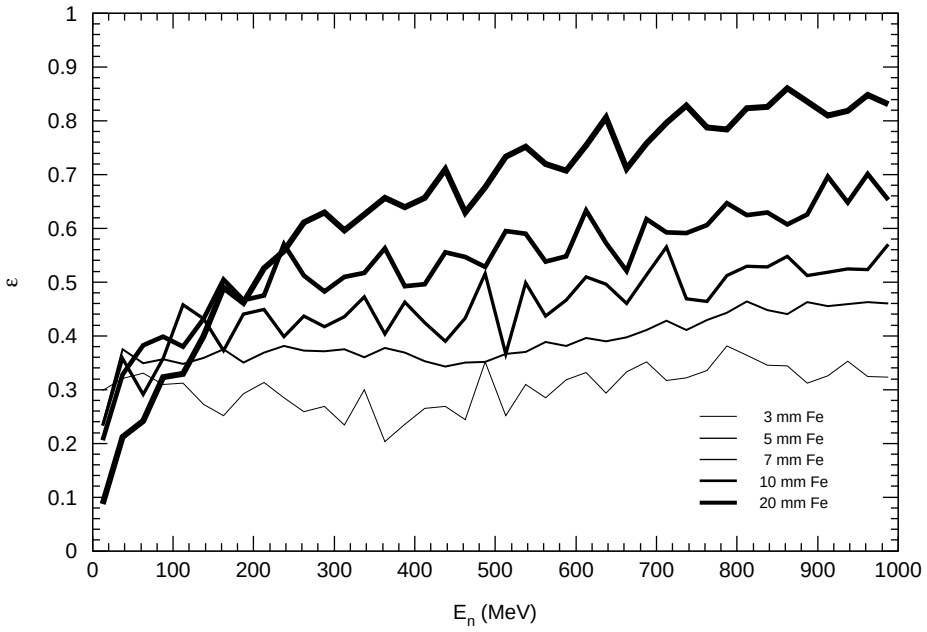

Figure 16: Efficiency curves for a 200×200 cm^2 sandwich structure consisting of 20 plastic scintillator sheets with 5 mm thickness each and 20 iron layers of different thicknesses (see legend).

a simulation this can be tricky. For example, for the HETC simulations of a $200 \times 200 \times 20$ cm^3 detector described in Ref. 2, it is not specified how many PM tubes are used and how the light is summed up, or if the scintillator is divided in separate paddles or not. These things, however, can change the shape of the efficiency curve significantly. Another point that is not clear is how the light attenuation was taken into account. For the calculations presented earlier in this report, light attenuation was not taken into account since it is unclear how the PM tubes are mounted to the hypothetical detector. Figure 17 shows the effect of light attenuation. For the simulations with light attenuation, the horizontal distance to the left and right side of the detector was used to determine the attenuation.

The effect of the light attenuation is most visible for the iron-scintillator sandwich structure, while it does not largely change the efficiency for the pure scintillator configuration at higher neutron energies. It should be noted that for this simulation, the light output of complete 2×2 m^2 panels was taken, without dividing into separate paddles as would be done for a real detector. The effect of a division in terms of efficiency, however, is very small.

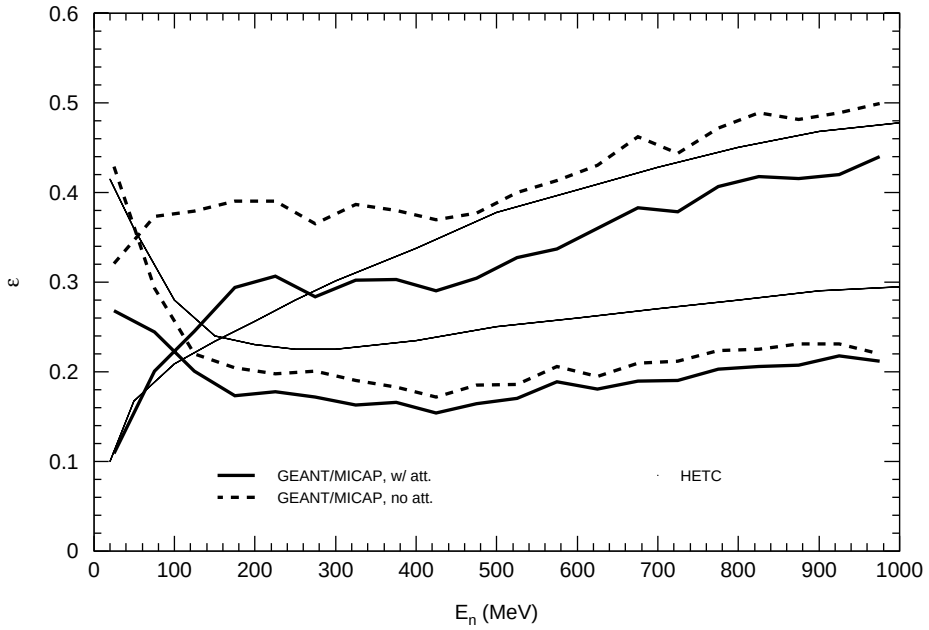

Figure 17: This figure shows two sets of efficiency curves calculated by GEANT with (thick solid) and without (thick dashed) taking light attenuation into account. One set corresponds to a $200 \times 200 \times 20$ cm^3 pure plastic scintillator (lower curves), while the other simulates a $200 \times 200 \times 20$ cm^3 iron-scintillator sandwich structure. The results of HETC simulations from Ref. 2 are shown for comparison.

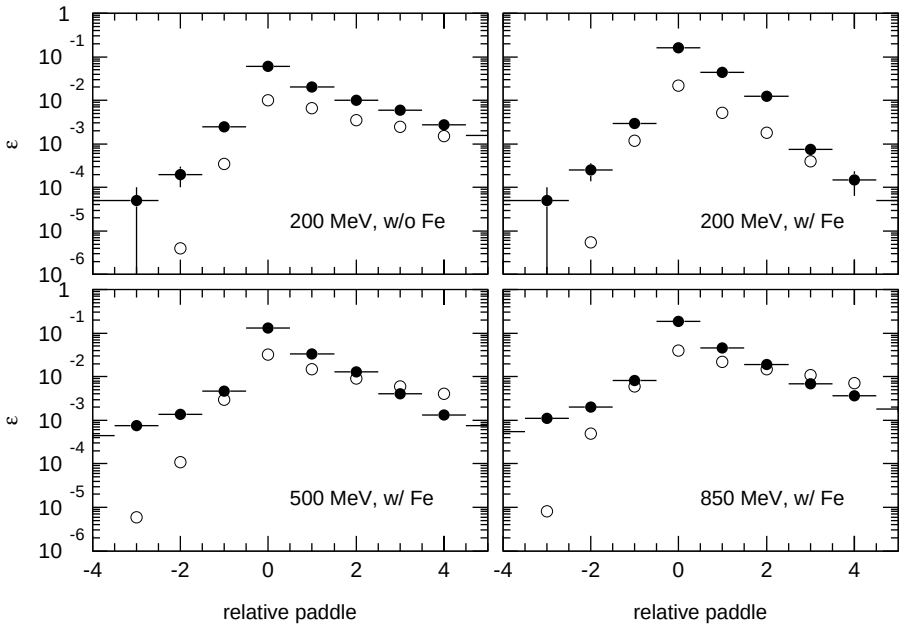

Figure 18: Efficiencies of an eight-paddle setup according to a measurement at SATURNE [2], and calculated by GEANT. Paddle 0 is the one that fired first, the other paddles are numbered with respect to paddle 0.

2.2.5 Comparing GEANT and the SATURNE measurements

The only measurements (to my knowledge) of neutron detection efficiencies for a combination of iron and scintillator were done by the LAND group. Part of the results are published in Ref. 2, but a more detailed description of the results would have been nice.

One of the measurements determined the relative efficiency of different paddles in a stack of eight, normalized to the paddle that first detected the neutron. The paddles are 50×9 cm^2 each with a thickness of 1 cm. Iron converters of 1 cm thickness were used. The first paddle served as a veto detector only. The results of this measurement are difficult to compare to simulations for two reasons: Firstly, it is not simple to define in a simulation which paddle fires first, and secondly, the absolute values of the simulated efficiencies seem to be lost (compare Fig. 1, Ref. 2). Fig. 18 shows the comparison of the measurement with the GEANT simulation for different energies and also without the iron in one case.

While the overall agreement of the *shape* is much better than the GEANT calculation presented in Fig. 1 of Ref. 2, the absolute numbers are off by far. However, with the complicated character of this measurement, I am not completely confident that the simulation I did really describes the measurement.

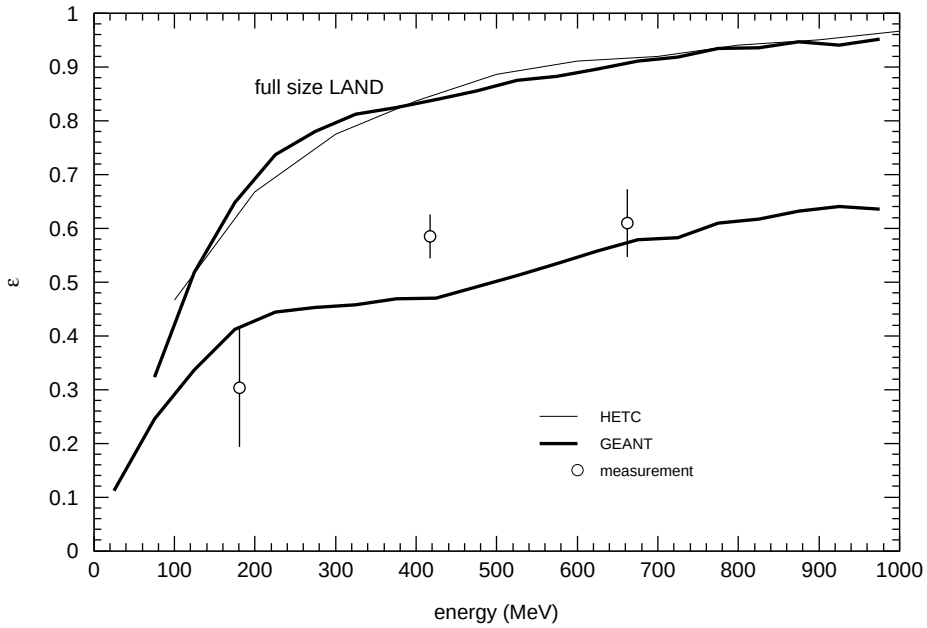

Figure 19: Measured efficiency of a test-setup for tagged neutrons at three energies (open circles) [2] in comparison with the GEANT simulation (filled circles). Also shown are simulations for the complete LAND setup. The HETC simulation taken from Ref. 2 (thin line) agrees well with my GEANT/MICAP simulation.

A much better test is provided by the measurement that was done with 10 prototype test paddles of the LAND detector using tagged neutrons from the SATURNE accelerator [2]. The neutron energies were 181, 417, and 662 MeV. Fig. 19 shows the three measured points in comparison with the GEANT simulation that I performed. The agreement between these two datasets is much better than in comparisons with the HETC simulations. Especially, at the lower energies, there is no large over-prediction of efficiency.

Reference 2 also shows efficiency curves that were predicted for the complete LAND detector using HETC and GEANT/GEISHA. These two simulations do not agree well. The GEANT/MICAP simulation I undertook, however, closely follows the HETC efficiency curve, as can be seen in Fig. 19.

3 Test measurement at RIKEN

The possibility of a test measurement at the RIKEN Accelerator Research Facility was discussed. The basic concept of this experiment will follow the efficiency measurement of a BaF_2 undertaken by R.A. Kryger et al. [8].

Neutrons of a broad energy range are produced using a 100 MeV/nucleon beam of ^{13}C impinging on a thick target. The primary beam is stopped in the

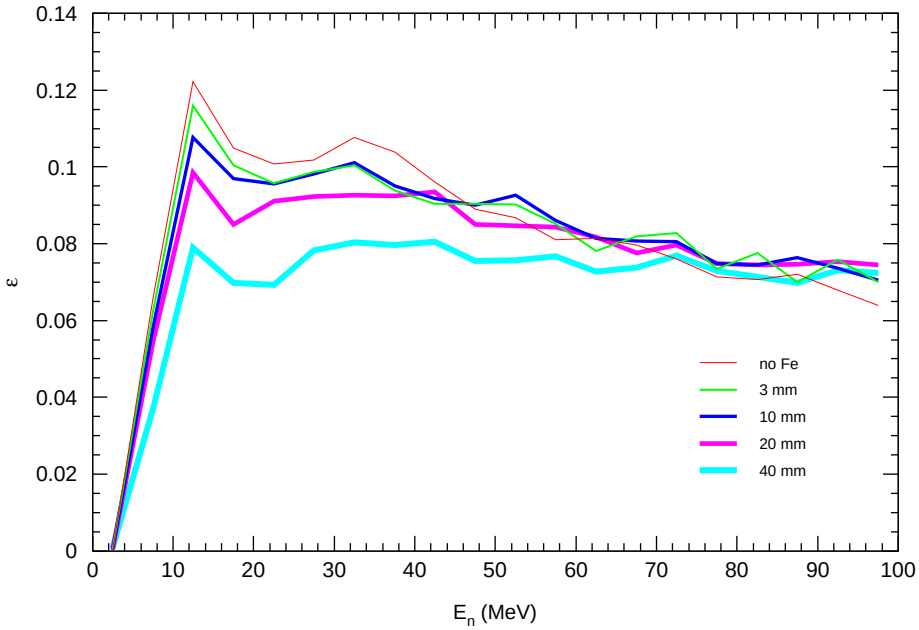

Figure 20: Simulated efficiency curves for a possible RIKEN test setup consisting of a 5 mm thick veto detector and one 6×6 cm bar from the RIKEN neutron wall. The different efficiency curves show the influence of the iron converter thickness.

target, so that only lighter fragments and neutrons can reach the detector setup. The neutron detectors are mounted at a distance of about 5 m from a start detector and the production target. This distance is needed in order to yield a sufficient energy resolution by a time-of-flight measurement. Two detector sets which are placed symmetrically with respect to the beam axis are employed.

RIKEN's neutron wall consists of blocks $6 \times 6 \times 108$ cm^3 with one PMT on each end. Each detector set consists of a thin veto detector and three blocks of the RIKEN neutron wall. An iron converter is placed in front of the neutron detector blocks in one of the two sets. The other set without the iron converter provides a reference detector for the efficiency, since the efficiency of plastic scintillator is well-known [5] and there are reliable programs to calculate this. The two detector sets are mounted symmetrically with respect to the beam axis, enabling a simultaneous measurement of the reference efficiency (see Fig. 21).

Separation of beam-related γ rays and neutrons can be achieved via a time-of-flight measurement. The time resolution of the neutron detector is approximately 100 ps. The background of cosmic γ rays can not be removed because plastic scintillator does not have pulse shape discrimination capabilities. However, with an intense neutron flux this is not a problem.

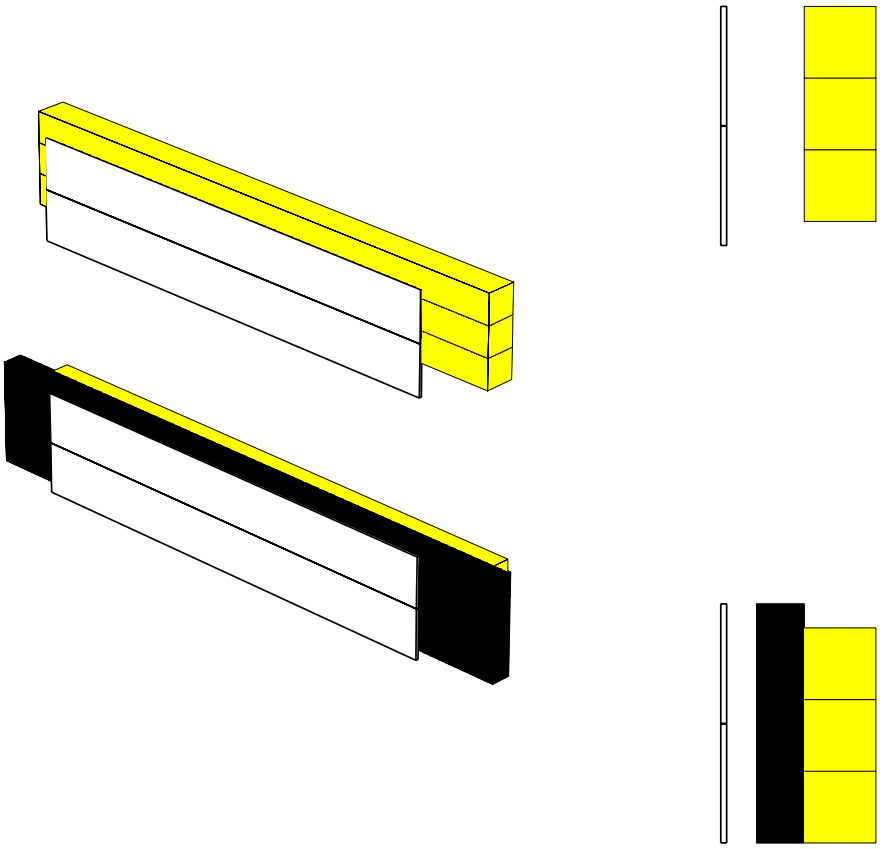

Figure 21: Schematic setup of the test experiment at RIKEN.

Figure 20 shows calculated efficiency curves for neutrons up to 100 MeV, that were obtained in a GEANT simulation. The setup consisted of a 5 mm veto detector and one 6 cm thick neutron detector bar. These simulations were done taking light attenuation in the plastic material into account and using a 2 MeVee threshold setting, applied to the light output on each end of the detector bar.

An iron converter of various thicknesses was added. The curves show that the efficiency can not be improved by large in this energy range and with this setup. However, there is a cross-over at roughly 120 MeV, above which the setup with 5 mm converter yields a slightly larger efficiency than the setup without converter.

A more subtle comparison can be achieved by plotting the ratio between two symmetric detectors, one with and one without the iron converter. This is the way it is done in the test experiment, where a detector without con-

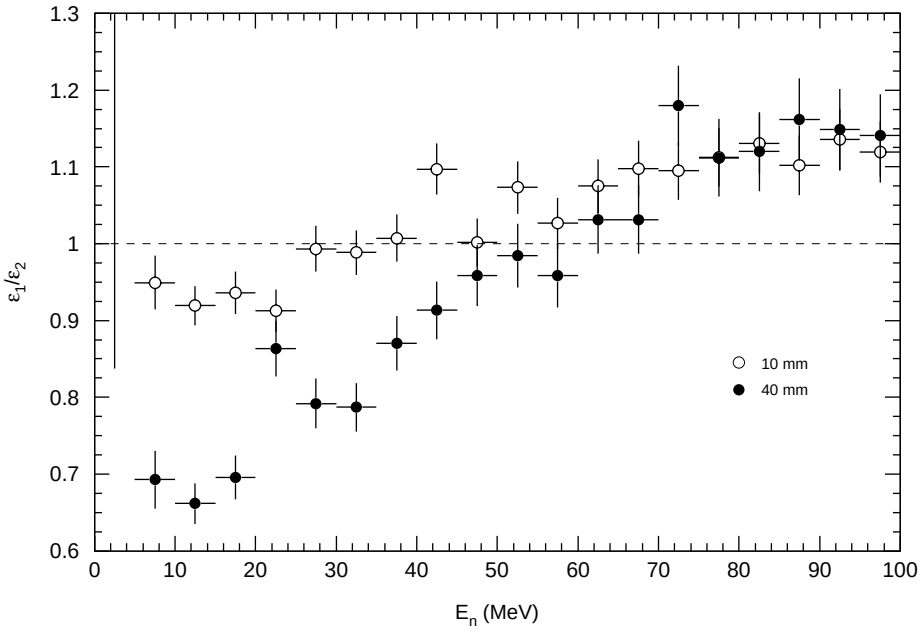

Figure 22: Ratio of detection efficiencies of the detector set with an iron converter in relation to that without the iron. This simulation was done using two different thicknesses of iron converter.

verter serves as a reference. For the simulation displayed in Fig. 22, the anticipated setup for this test experiment was modeled in GEANT, and the function of the veto detector was also taken into account, meaning that events where a neutron is detected in the veto detector or where a charged particle scatters back into the veto detector, are discarded.

3.1 Details of the test experiment

On November 22, 2000, a test experiment as described in the previous section is conducted at the RIKEN ring cyclotron using a ^{13}C beam of 100 MeV/u. The detector setup consists of two sets with 3 blocks $6 \times 6 \times 108$ cm^3 plastic scintillators each, mounted horizontally about 43 cm above and below the beam axis. The time-of-flight is measured between a start scintillator and the neutron detector along a flight path of 5.25 m in horizontal projection. Each of the scintillator blocks of the neutron detector is read out by one PMT on each side, giving a position resolution of roughly one centimeter. Plastic scintillator veto counters with 3 mm thickness are placed in front of each of the detector sets. The veto counters cover an area of 100 by 20 cm^2.

Between the veto counters and the neutron detectors is a gap of about 3.5 cm. For the lower of the two detector sets, this gap is filled with three steel plates of 1 cm thickness that serve as a converter.

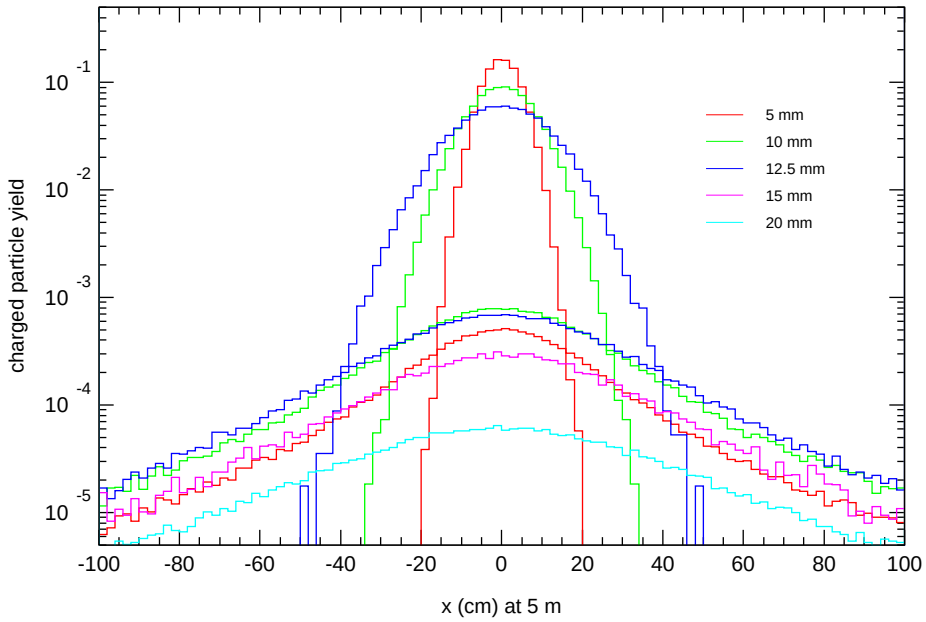

Figure 23: Yield of charged particles and their position distribution 5 m behind an aluminum reaction target (MOCADI simulation) with a beam of ^{13}C at 100 MeV/u impinging onto it. The narrow distributions correspond to ^{13}C projectiles for different thicknesses of aluminum targets. The wider distributions are the sum of all fragments. For 15 mm and 20 mm targets, the ^{13}C beam stops in the aluminum.

In a first measurement, the relative detection efficiencies of the detector set with converter and of the detector set without converter are determined. In a second measurement, the converter will be removed from the lower detector set and the efficiencies of the two sets are compered. Although the setup is symmetric, the two detector sets are not identical and differences in detection efficiency have to be corrected.

4 Design

This detector will be designed by following a list of criteria which seem necessary for a good performance. These criteria are:

- high detection efficiency between 50 and 300 MeV neutron energy.
- good time resolution.
- granularity corresponds to neutron scattering.
- simplicity and economy.

4.1 Adopt LAND design to lower energies

The LAND design with its homogeneously distributed iron converter sheets yields very high detection efficiencies for high-energy neutrons. Simply by removing the iron converters from the first paddles, the efficiency for lower energies can be improved. Furthermore, it is questionable if the complicated sandwich structure consisting of 5 mm sheets of iron and scintillator is necessary. In a first attempt, I used the same paddle dimensions of $200 \times 10 \times 10$ cm^3, but without any iron converters. Iron converters of 3 cm thickness are inserted in front of the second half of 10 paddle layers (see left side of Fig. 24). It should be noted that the resulting detector is 15 cm longer than LAND, because I added the iron to the pure scintillator paddles. Nevertheless, the efficiency for energies below 170 MeV is much better!

4.2 How does the converter work?

The impinging neutrons interact in the converter material with a higher probability due to the shorter nuclear interaction length. Charged particles that are created in these interactions leave the converter and can then be detected in the scintillator. According to the GEANT simulations, protons play the most important role.

I produced lists that give the number of different particles which deposit energy in the scintillator, normalized to the number of neutrons that enter the detector. Tables 1 and 2 show these numbers.

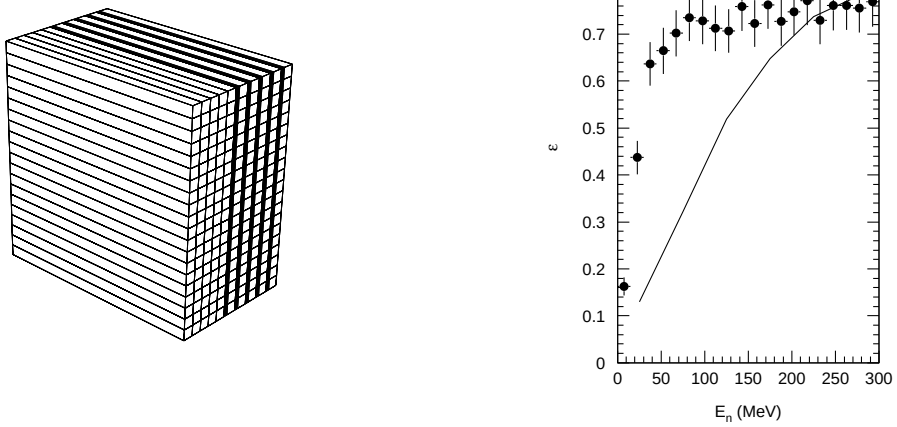

Figure 24: Detector consisting of 200 $200 \times 10 \times 10$ cm^3 pure scintillator paddles and five layers of 3 cm iron converter (black). The efficiency curve is shown on the right (filled circles) and compared to that of LAND (line).

Table 1: This table lists the number of particles that are created and deposit energy in the scintillator for each neutron that enters the detector. Following numbers apply to a single $200 \times 10 \times 10$ cm^3 scintillator bar with 10 cm iron converter, 200 MeV neutrons.

Particle	w/o converter	w/ converter
γ	0.021	0.047
e^-	0.021	0.063
p	0.161	0.341
α	0.087	0.083
efficiency	0.085	0.12

Table 2: This table lists the number of particles that are created and deposit energy in the scintillator for each neutron that enters the detector. Following numbers apply to a single $200 \times 10 \times 10$ cm^3 scintillator bar with 10 cm iron converter, 200 MeV neutrons.

Particle	w/o converter	w/ converter
γ	0.021	0.047
e^-	0.021	0.063
p	0.161	0.341
α	0.087	0.083
efficiency	0.085	0.12

Table 3: Same numbers as described in Table 1, but for a wall of 20 200 × 10 × 10 cm^3 scintillator bars with 4 cm iron converter, 300 MeV neutrons.

Particle	w/o converter	w/ converter
γ	0.051	0.089
e^-	0.03	0.15
p	0.22	0.447
α	0.09	0.125
efficiency	0.069	0.15

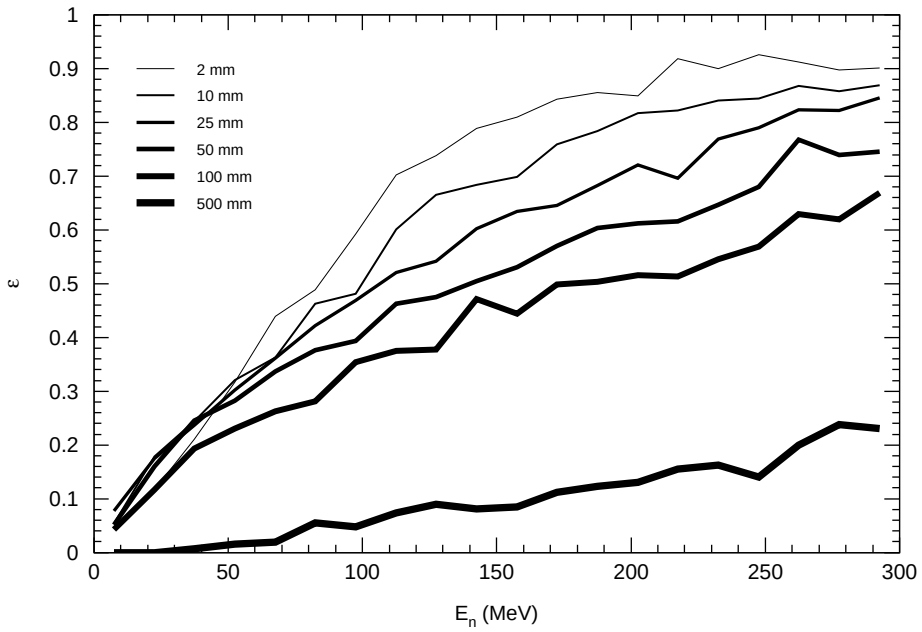

Figure 25: Efficiency curves for a 200 × 200 × 100 cm^3 block of alternating layers of iron and scintillator. The different curves correspond to a variation in layer thicknesses. The differences of light collection with varying thickness of the scintillator were not taken into account for this simulation.

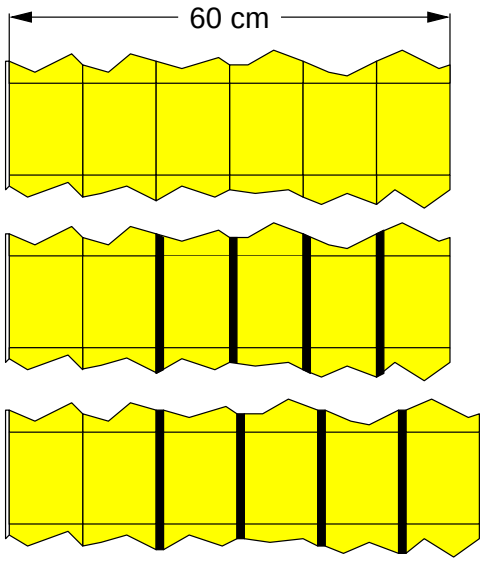

Figure 26: Different layouts of pure scintillator and a combination of scintillator and iron converter. The resulting efficiency curves are shown in Fig. 27.

4.2.1 The converter thickness

As already pointed out in Ref. 2, the optimal distribution of scintillator and converter would be in very thin alternating layers, so that all charged particles that are produced in the converter can exit the converter. The thickness of the converter and scintillator layers, which is practical, is off course limited by other considerations, most notably the light collection.

4.2.2 Comparison of a detector with and without converter

A key question when adopting a passive converter for lower energy neutrons is at which energy the converter makes sense, i.e. at which energy does the converter enhance the detection efficiency. In order to investigate this, a comparison of detection efficiencies for a pure scintillator and a scintillator/converter combination with the same detector volume was done.

The different layouts that were simulated for this comparison are drawn in Fig. 26. The resulting efficiency curves are plotted in Fig. 27. While the passive converter reduces the detection efficiency for a small range of energies below 75 MeV, it significantly enhances efficiency for neutrons with energies of 100 MeV and above.

4.3 Cost of the detector

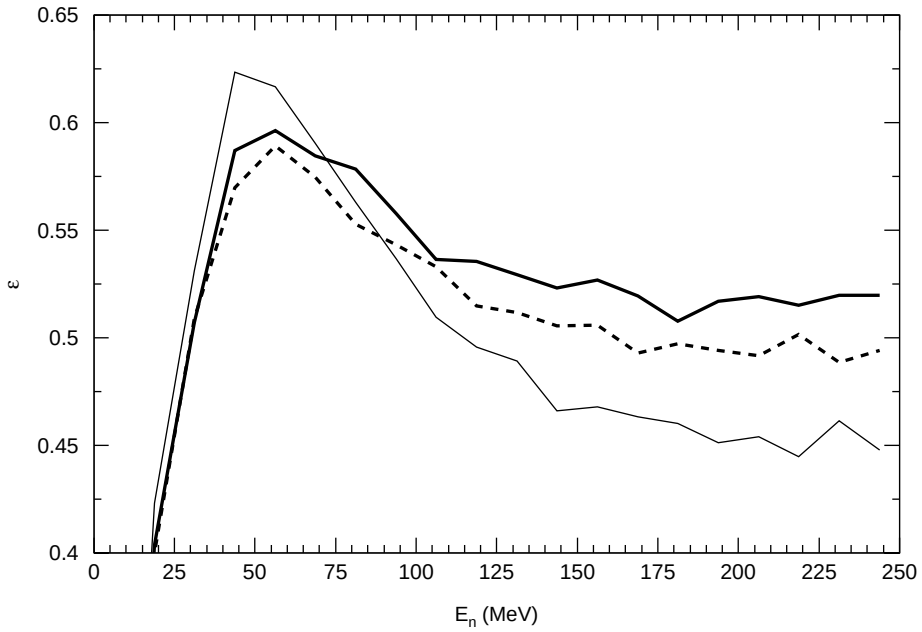

Figure 27: Efficiency curves for a 200×200 cm^2 detector consisting of one 5 mm veto detector block and six layers of neutron detector (see Fig. 26). The thin line represents a simulation with six 10 cm scintillator layers and no converter. The thick dashed line shows how the efficiency changes if the last four detector layers consist of 1 cm iron and 9 cm scintillator each, keeping the overall detector volume constant. Just adding the 1 cm iron converters to the last four layers, keeping the scintillator thickness at 10 cm, yields the thick efficiency curve.

References

[1] P.D. Zecher *et al.*, Nucl. Instr. & Meth. A 401 (1997) 329–344 1

[2] Th. Blaich *et al.*, Nucl. Instr. & Meth. A 314 (1992) 136–154 1, 2, 2, 19, 20, 20

[3] computer code GEANT 3.21, CERN Program Library, `wwwinfo.cern.ch/asd/geant` (1999) 1

[4] P.A. Aarnio *et al.*, Fluka user's guide, Technical Report TIS-RP-190, CERN (1987) 1990 2

[5] R.A. Cecil, B.D. Anderson, and R. Madey, Nucl. Instr. & Meth. 161 (1979) 439–447 2, 3, 4, 9, 21

[6] R.L. Craun and D.L. Smith, Nucl. Instr. & Meth. 80 (1970) 239–244

[7] Glenn F. Knoll, *Radiation Detection And Measurement*, 2nd edition (1989)

[8] R.A. Kryger *et al.*, Nucl. Instr. & Meth. A 346 (1994) 544–547 20